Colloid Polym Sci 279:498–505 (2001)

SHORT COMMUNICATION

E. Pefferkorn
E. Ringenbach
F. Elfarissi

Aluminium ions at polyelectrolyte interfaces. III. Role in polyacrylic acid/aluminium oxide and humic acid/kaolinite aggregate cohesion

Received: 24 July 2000
Accepted: 20 December 2000

E. Pefferkorn (✉) · E. Ringenbach
F. Elfarissi
Institut Charles Sadron
6 rue Boussingault
67083 Strasbourg Cédex, France

Abstract Understanding the formation and breakup of humic acids and clays agglomerates is a difficult challenge owing to their complex nature. Thus, to progress in the study of the stability of such systems, attempts were made to replace the humic acid/kaolinite natural system by the polyacrylic acid/aluminium oxide synthetic system. Since the present investigation was dedicated to determine some characteristics of acidic soils which contain traces of aluminium ions, these ions were added to the adsorbent/polyacid systems as trace constituents. Initial and short-term phenomena related to the adsorption of humic and polyacrylic acids on aluminium oxide and kaolinite clay have been presented elsewhere. Here we present long-term phenomena regarding the formation and cohesion of oxide and clay aggregates formed in the presence of polyacrylic and humic acids, respectively. The results of electrophoretic mobility measurements demonstrated the amphipathic character of polymeric layers adsorbed on aluminium oxide and the amphoteric character of humic acid layers adsorbed on kaolinite. The long-term stability of the two colloidal systems was determined to evolve similarly despite the existence of the these typical characteristics.

Key words Cohesion of polyacrylic acid/oxide complexes · Cohesion of humic acid/kaolinite complexes · Amphipatic polymer layer · Amphoteric polyelectrolyte layer

Introduction

Agricultural soils are composed of agglomerates of clays and particulate matter of various sizes and shapes, of crystalline or amorphous nature [1]. The cohesion of soil aggregates results from combinatory effects of inorganic and organic materials. The latter constituents were determined to be responsible for the stability of agglomerated fine particles, such as oxides and clays, which in turn ensure the cohesion of the ensemble on larger scales [2, 3]. The ionic composition of soils depends on a great number of parameters and we were especially interested in studying the effects of aluminium ions which remain as the major ionic component of acidic soils, when other ions of smaller valence have been washed out by acid rain [4, 5]. In order to progress in the understanding of the cohesion of soil agglomerates, we first investigated a synthetic system (polyacrylic acid/aluminium oxide) before extending the investigations to a natural system (humic acids/kaolinite clay).

The objectives of the present work were to investigate the internal cohesion of organic/inorganic agglomerates and to interpret the long-term stability in terms of electrochemical characteristics of the ternary systems constituted of the solid particles, the macromolecules and the aluminium ion. Different methods of investigation of the stability and cohesion of soil aggregates have been described in the literature. Chaney and Swift [6] determined the existence and extent of any correlation between the aggregate stability and the various soil

properties or components involved in soil aggregation. The aggregate stability was assessed by a wet-sieving technique and the results were presented as a mean-weight-diameter value, which was calculated by multiplying the weight of the soil on each sieve by the mean intersieve size. The procedure thus provided values between 25 and 240 for completely unstable and very stable aggregates, respectively. Highly significant correlations were obtained for the relationships between aggregate stability and organic matter content. No other soil constituent investigated had a significant relationship with aggregate stability, indicating that organic matter was mainly responsible for the stabilisation of the aggregates. In a second set of experiments, Chaney and Swift [7] determined the ability of humic substances to restructure the dispersed soil. Care was taken to employ inorganic and organic matter for which multivalent ions had been removed. The stability of aggregates following adsorption was close to 134 after 14 days incubation, while that without humic substances was 27. Interestingly, when the humic material was added to the soil, either in an insoluble form (calcium humate) or in a soluble form which is precipitated on addition to the soil (sodium humate on a calcium soil), very little stabilisation of the aggregates was determined to have been established. The authors concluded that aggregate stability seemed to result only from the adsorption and not from the interfacial precipitation of insoluble material.

In the present study, the complex role of aluminium ions on the rate of aggregation/breakup of organic/inorganic agglomerates was studied by determining the mass distribution curves of the colloids and by deriving the average masses of the agglomerates as a function of time. This was done since the mass distribution function was determined to allow determination of the rate of aggregate breakup, and on the basis of theoretical and/or numerical models, provides information on the breakup mechanism [8–11].

Materials and methods

The (synthetic) aluminium oxide/polyacrylic acid system

The α-alumina samples of industrial origin (Aluminium-Péchiney) were partially soluble at pH 5 and contained different major impurities, such as Na_2O, SiO_2, Fe_2O_3 and CaO. Ca (0.1%) could be fully extracted while Mg (0.3%) remained after treatment in acidic or salt media. The alumina particles had a mean size of 1.54 μm, and a specific surface area determined from the Brunauer–Emmett–Teller adsorption isotherm of 3.0 m^2/g. The dissolution in 10^{-3} mol/l aqueous KCl solution of the aluminium oxide provided 10^{-4} mol/l aluminium ions at the equilibrium pH of 5.0. Surface and solute aluminium ions were determined to interact with polyacrylic acid (of molecular weight 9.6×10^5), giving rise to a hydrophobic thin layer on the oxide surface and an adjacent polymeric layer composed of positively, negatively and neutral chain segments [12], thus building a very complex amphoteric layer [13].

The (natural) kaolinite/humic acid system

The bare clay was a kaolinite-type material of French origin (Kaolin des Charentes, code type name GZA IV) and the morphological, chemical and surface area characteristics are given in Ref. [13]. The clay was suspended in aqueous solution at pH 3.5 (0.5 g/l) and fractionated by two sedimentation procedures. Particles of very large sizes were allowed to settle out by gravity and discarded, this operation being repeated five times. Particles of very small sizes were discarded after the second sedimentation run by removing the upper portion of the suspension and this operation was also repeated five times. This sample was used in the fragmentation study and was analysed for mass and size distributions using a Coulter counter and a Coulter laser diffractometer, respectively [14]. The resulting mass and size distributions evidence that all the suspended grains of the fractionated sample can be detected and are counted by the particle counter when they are suspended at pH 5. This precaution ensures that practically no detectable grain or aggregate originates from agglomeration of "invisible" shattered matter or that clay particles of diameter smaller than 0.9 μm constitute weak cohesive interaggregate links. The volume-average diameter, d_h, was determined to be 1.3 μ. Clay doses are expressed by the weight of kaolinite suspended in 100 g of suspension.

The peat-derived humic substance was supplied as sodium humate by Aldrich Chimie and some characteristics are given in Ref. [13] The humate powder dissolved in water gave an alkaline solution of pH 8 and the nonsoluble constituents were centrifuged. Stock solutions at a concentration of 1 g/l in 10^{-3} mol/l aqueous KCl solutions at pH 5.0 appeared coloured. Acid–base titration of the humic acids showed the equivalent concentration of acid groups to be 0.003 mol/g. Turbidity measurements at 500 nm on solutions at varying polymer concentrations showed the organic substance to be soluble in aqueous solution at pH 5 and 25 °C in the presence of aluminium ions below a threshold concentration of 2×10^{-4} mol/l of $AlCl_3$.

Aluminium ions were added to the kaolinite suspension to get a virtual concentration of 10^{-4} mol/l. Owing to ion-exchange processes with counterions of anionic sites generated by the isomorphous substitution [15] and subsequent adsorption of aluminium ions at the kaolinite surface, the concentration of the residual aluminium ions available for polyacid complexation became smaller and depends on the clay dose as shown in Fig. 1.

Adsorption of aluminium ions on kaolinite clay promotes the change in the net surface charge as evidenced from the passage of −17 mV (bare clay) to 15 mV when the adsorption is a maximum. The modified clay interacts with humic acid and the resulting adsorption layer undergoes long-term modifications. Additional information obtained from Fig. 1 is that when the ratio of the concentration of humic acid and that of residual aluminium ions is modified by changing the clay dose or the humic acid concentration, this may induce different interfacial structures and behaviour. The polyelectrolyte behaviour was determined to occur at high clay doses and humic acid concentration, while the polyamphoteric behaviour was determined to occur at small doses and humic acid concentration [16]. Additionally, changing the kaolinite dose promotes clay surfaces with different aluminium ion densities as induced by the selective ion-exchange process when the relative ion concentration in the liquid phase is changed according to the results of Fig. 1.

Electrophoretic mobility

Measurements of electrophoretic mobility of the bare, complexed and polyacrylic or humic acid coated kaolinite and alumina particles were carried out using a Malvern Zeta Sizer III. In all situations, the experiments were carried out at 25 °C. The precision and accuracy of the experimental results were checked using a

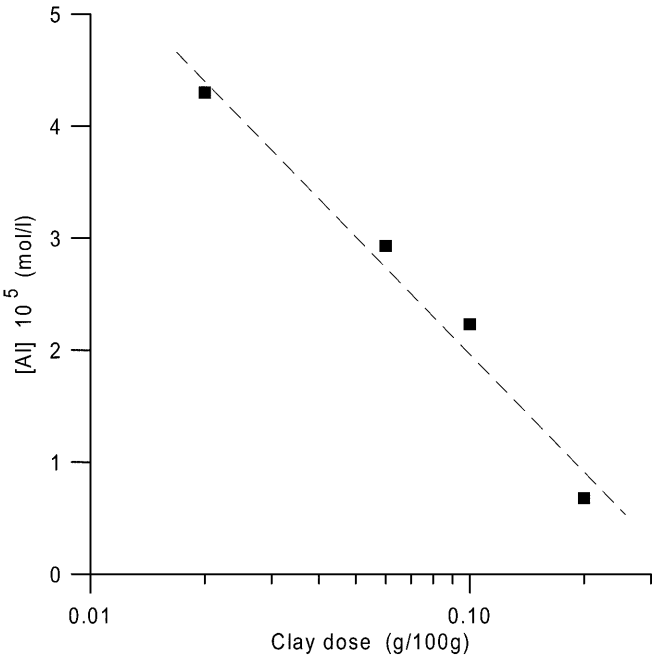

Fig. 1 Residual aluminium ion concentration as a function of the kaolinite clay dose (log scale) after immersion of clay doses in 50 ml aqueous (10^{-4} mol/l $AlCl_3$, 10^{-3} mol/l KCl and 10^{-5} mol/l HCl) solution

standard colloid suspended in a given standard buffer, for which the mobility should be reproduced with an error smaller than $\pm 10\%$. The problem of accurately measuring the mobility of slow particles was by modulating one of the laser beams. Changes in the electrophoretic mobility were expressed by changes in the ζ potential as determined using Smoluchowski's equation.

Reduced mass characteristics of aggregates

The progress of the aggregation or the fragmentation processes was determined from the variation with time of the number-average, $N(t)$, and weight-average, $S(t)$, masses of the aggregates or fragments defined by

$$N(t) = \frac{\sum_n nc(n,t)}{\sum_n c(n,t)},\ S(t) = \frac{\sum_n n^2 c(n,t)}{\sum_n nc(n,t)}. \quad (1)$$

$N(t)$ and $S(t)$ were calculated from the aggregate mass distribution, $c(n,t)$, derived from the histogram given by the particle counter [17–20]. For a monodisperse agglomerate containing n particles the Coulter counter provided the volume concentration of spheres of volume $\pi d_n^3/6$ equal to $n\pi d_1^3/6$ of the volumes of the n particles, as if all the n particles were collapsed in one compact sphere. The mass, n, was then obtained using the following relationship:

$$n = (d_n/(d_1))^3. \quad (2)$$

To determine the characteristics of the polydisperse colloidal systems, the experimental variation, $V(i)$, of the average concentration for each channel i was subdivided into $v(i)$ concentration intervals, the width of each interval representing the increase in diameter of the collapsed equivalent sphere resulting from the addition of one single particle to the previous aggregate [21]. This procedure transforms the crude histogram given by the particle counter into the corresponding mass distribution curve, $c(n,t)$ versus n.

For aluminium oxide and kaolinite particles the mass $S = 1$ was attributed to particles of apparent volume-average harmonic diameter of 0.79 and 1.3 μm, respectively. The value of 0.79 μm corresponded to the apparent diameter of the smallest grain present in the system. Larger grains were thus considered as being compact agglomerates of these grains and the average masses $N(t=0)$ and $S(t=0)$ for the dispersed system were determined to be 27 and 87, respectively. For the kaolinite particle the value of 1.3 μm corresponded to the diameter of a sphere of volume equal to that of the clay platelets present at the maximum concentration. Owing to the morphology and size characteristics of the clay, we cannot further consider large clays as being agglomerates of identical platelets since both the thickness and the diameter of the platelets are different actually. The choice of the first or the second definition for the single particle characteristics actually led to different values of $N(t)$ and $S(t)$ but did not affect the exponents of the power laws expressing the kinetics of the aggregation or fragmentation processes.

Theoretical basis

Aggregate fragmentation was first taken into account in reversible aggregation processes when, after being formed, one or several intraaggregate links were disrupted. The predicted effects are to reduce the aggregation rate and, in many instances, to install an aggregation/fragmentation steady state [22, 23]. Additionally, the process may induce aggregate compaction [24–26]. The fragmentation process itself is assumed to develop at random according to the following reaction [8–11, 27–29]:

$$A_y \xrightarrow{B(i,j)} A_i + A_j, \quad (3)$$

where the rate constant of the fragmentation process $B(i,j)$ is given by

$$B(i,j) = k(i+j)^{\alpha}. \quad (4)$$

According to Eq. (1), two extreme fragmentation modes are taken into account, which accord with two typical variations of the weight-average and number-average masses as a function of time:

On the basis of a given decrease in $N(t)$ with time, when $i \ll j$ $S(t)$ is expected to decrease relatively slowly to account for the slow disappearance of the largest aggregates, whereas when $i \cong j$ $S(t)$ is expected to decrease relatively strongly to account for the fast disappearance of aggregates of large sizes. Similarly, the fragment polydispersity $S(t)/N(t)$ is expected to be constant when $i \ll j$ and to decrease strongly when $i \cong j$. It is therefore interesting to determine the temporal evolution of the mass polydispersity $S(t)/N(t)$.

We present elements of the recent theory of fragmentation, which uses the integrodifferential Eq. (5) to describe the fragmentation rate [9]:

$$\frac{\partial c(n,t)}{\partial t} = -a(n)c(n,t) + \sum_{y=n}^{\infty} c(y,t)a(y)f\langle n|y\rangle, \quad (5)$$

where $c(n,t)$ is the concentration of aggregates of size n at time t, $a(n)$ is the rate of breakup of the aggregate of size n during time ∂t and $f(n/y)$ is the rate at which aggregates of size n are produced from the breakup of clusters of size y. In the theory of Cheng and Redner [9, 10], homogeneous kernels of the form

$$a(\mathrm{n}) = n^{\lambda} \tag{6}$$

and

$$f\langle n|y\rangle = y^{-1} b\langle n|y\rangle \tag{7}$$

were considered. The rate, $b(n)$, of formation of fragments of size n from aggregates of size y is thus expressed by

$$b(n) = n^{v}. \tag{8}$$

The treatment of Eq. (5) was carried out on the basis of the usual reduced form of the mass frequency given in Eq. (9):

$$c(n,t)S^2(t) \propto f[n/S(t)]. \tag{9}$$

Both $a(n)$ and $b(n)$ can be derived from the cluster size distribution. Cheng and Redner demonstrated that the rate of fragmentation of aggregates of size n, which is measured by the exponent λ, may be calculated from the variation of the function $\varphi(n)$ for $n/S(t) > 1$. This may be understood if one considers the change in the concentration of the large colloids to be highly affected by the fragmentation of the largest aggregates. This leads to

$$\varphi\left(\frac{n}{S(t)}\right) \approx c(n,t)S^2(t) \approx n^2 \exp\left[-a\left(\frac{n}{S(t)}\right)^{\lambda}\right]. \tag{10}$$

On the other hand, the rate of formation of aggregates of small size can be derived from the slope of the function φ at small values of the variable $n/S(t)$. Qualitatively, the size distribution of the smallest aggregates is expected to be imposed by the rate $b(n)$ of aggregates of mass y larger than n. Thus, the rate of formation of small fragments, $b(n)$, is measured by the value of the initial slope of the function $f(n)$ for $n/S(t) < 1$ as

$$\varphi\left(\frac{n}{S(t)}\right) \approx \left(\frac{n}{S(t)}\right)^{v}. \tag{11}$$

The shape of the colloid size distribution during the fragmentation process thus determines the nature and the rate of fragmentation. The mass frequency also allows the average sizes $S(t)$ and $N(t)$ to be calculated and, for the model of Cheng and Redner [9, 10], their temporal variation is given by

$$S(t) \approx N(t) \approx t^{-1/\lambda}. \tag{12}$$

Deviation from these simple irreversible fragmentation processes may occur, and in order to take into account the possible concomitance of different fragmentation processes when the mass polydispersity is found to vary with time, we introduced Eq. (13) to characterise separately the variation of $N(t)$ [30]:

$$N(t) \approx t^{-1/\mu}. \tag{13}$$

In the case of coagulation/fragmentation models, which means that fragments may recombine to form an aggregate of greater mass, Ernst and van Dongen [11] determined the following expression for the rate of variation of $S(t)$:

$$S(t) \approx t^{1/v}. \tag{14}$$

Results and discussion

Electrokinetic characteristics of charged interfaces

Different characteristics (concentrations of the polymer and aluminium ions in the supernatant, pH of the suspension and electrophoretic mobility) were determined at 24 and 1000 h for suspensions of aluminium oxide/polyacrylic acid complexes maintained under slow stirring. The electrophoretic mobility was determined for suspensions of kaolinite/humic acid complexes at 24 and 168 h maintained under slow stirring. After 1000 and 168 h, respectively, the synthetic and the natural systems have more or less recovered the dispersed state which existed at time zero. Although no variation in the polymer and aluminium ion concentrations was determined to occur [31], changes in the electrophoretic mobility were observed as reported in Figs. 2 and 3 for the synthetic and natural systems, respectively.

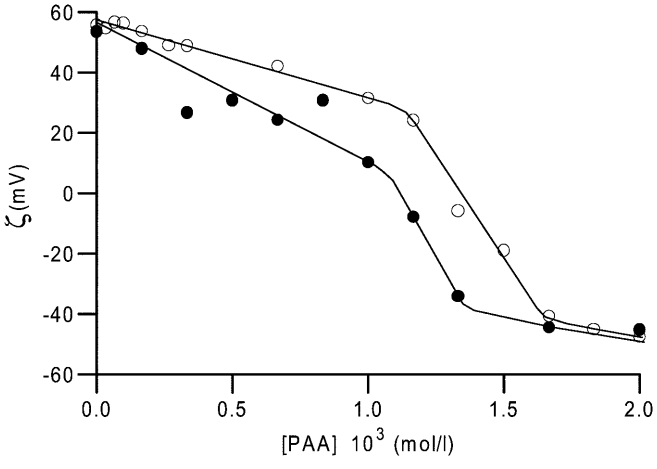

Fig. 2 ζ potential of bare aluminium oxide particles and of aluminium oxide/polyacrylic acid (*PAA*)/aluminium ion complexes as a function of the initial PAA concentration determined at 24 h (○) and 1000 h (●)

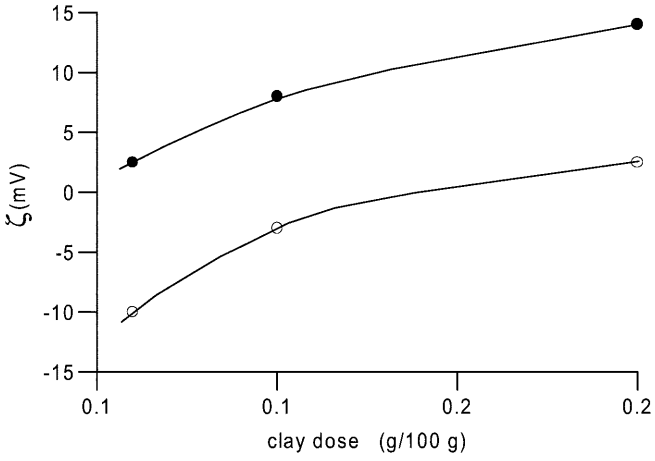

Fig. 3 ζ potential of kaolinite/humic acid/aluminium ion complexes as a function of the clay dose determined at 24 h (○) and 168 h (●) for systems characterized by the constant concentration in humic acid of 5 mg/l or 1.5×10^{-5} mol/l

Long-term modifications induced by adsorption of polyacrylic acid at the oxide surface

As depicted in Fig. 2 the ζ potential shifts towards lower values at all polymer concentrations below a threshold value close to −50 mV, which corresponds to the adsorption of noncomplexed polyacrylic acid. The difference in mobility at 24 and 1000 h is attributed to changes in the spatial distribution of neutral, positively and negatively charged chain segments. The resulting effect of the segregation is to decrease the mobility in the domain of small polymer concentrations, to inverse the particle flux in the domain of medium concentrations and to increase the mobility at higher concentrations. The global relative variation as a function of time should result from the assumption that the relative portion of negatively charged groups increases in the outer zone of the layer, whereas that of the positively charged groups increases in the inner zone [32, 33]. Therefore, the segregation should result from the combined effects of the hydrophobic character of the complexed chain segments and the hydrophilic character of the chain segments bearing dissociated carboxylic acid groups [34]. Actually, the greater concentration of hydrophobic moieties in the zone adjacent to the solid, where the chain segment density is high, allows energetically favourable segment–segment contacts. Conversely, the greater concentration of hydrophilic moieties in the outer layer, where the chain segment density is relatively low, allows energetically favourable segment–solvent contacts [35]. Additionally, this type of segregation accords with the locally neutral character of the thin skin resulting from complexation of the acid groups of the adsorbed polyelectrolyte by oxide surface sites as reported in Ref. [13]. The interfacial segregation induced by adsorption on the oxide is driven by the energy gain resulting from the segregated distribution of hydrophobic and hydrophilic moieties within the adsorbed polymer layer as represented schematically in Fig. 4a.

Long-term modifications induced by adsorption of humic acid at the clay surface

Similarly, charge segregation phenomena as a function of time were evidenced from modifications of the electrophoretic mobility of humic acid coated kaolinite clay. Figure 3 represents the ζ potential of the clay–aluminium ion–humate complex for systems characterised by a constant concentration in humic acid (5 mg/l or 1.5×10^{-5} mol/l) and different doses of kaolinite inducing initially different residual concentrations of aluminium ions. For the three experiments, from the consideration of the humic acid, the residual aluminium ion concentrations and the change arising in the pH of the suspension, we determined the aluminium ion modified kaolinite clay to develop very different surface charge characteristics, while the degree of complexation of the humic acid remained at the maximum value of 0.28 ± 0.02 (see Fig. 3 in Ref. [13] for details).

The most specific information is the change from negative to positive mobility as a function of time. This variation implies that the positively charged chain segments migrate towards the external zone of the layer and the negatively charged chain segments concentrate adjacent to the solid surface zone. The operative force of the charge segregation should be of an electric nature since the kaolinite-modified surface is positively charged.

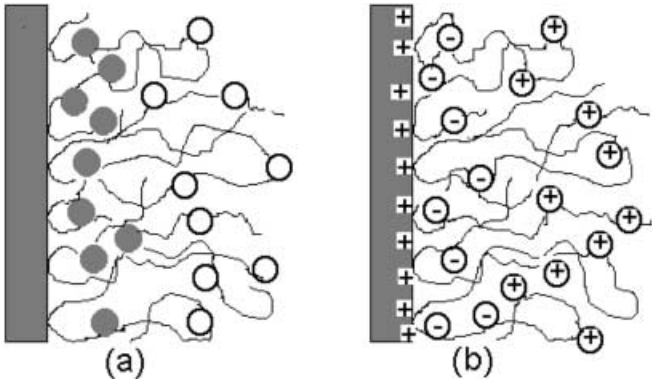

Fig. 4 Schematic representation of **a** the oxide-PAA and **b** the modified kaolinite-humic acid layers at adsorption equilibrium. In **a** ● and ○ represent the hydrophobic (complexed acid groups) and hydrophilic (neutral or dissociated acid groups) moieties on the PAA chain, respectively. In **b** + represents the positively charged sites on the kaolinite surface modified by adsorption of aluminium ions while ⊕ and ⊖ represent the positively (complexed) and negatively charged (dissociated) groups of the humic acid chain, respectively

Obviously, this is possible owing to the lower degree of complexation of the carboxylic groups since segregation on the basis of the existence of a great number of hydrophobic groups would have initiated the segregation in the inverse direction as was determined for the aluminium oxide situation. The equilibrium situation is schematised in Fig. 4b.

Stability of the colloid–polyelectrolyte complexes

The long-term behaviour was investigated for the aluminium oxide–polyacrylic acid and the kaolinite–humic acid systems and in all the situations the aggregates obtained in the presence of synthetic or natural macromolecules were found to fragment slowly and the initial dispersed systems were restored more or less after 1000 and 168 h for the synthetic and natural systems, respectively. The fragmentation rates, defined by the variation with time of $S(t)$ and $N(t)$, were found to obey power laws.

The number-average and weight-average masses are shown in Figs. 5 and 6 as a function of time (log–log scale) for the synthetic and natural systems, respectively. The variations with time of $N(t)$ and $S(t)$ are given in the figures to show the variation of the mass polydispersity, which is given by $S(t)/N(t)$. After mixing the systems become highly aggregated and this situation is maintained for 1 h for the synthetic system and for 10 h for the natural one, then the masses of the aggregates

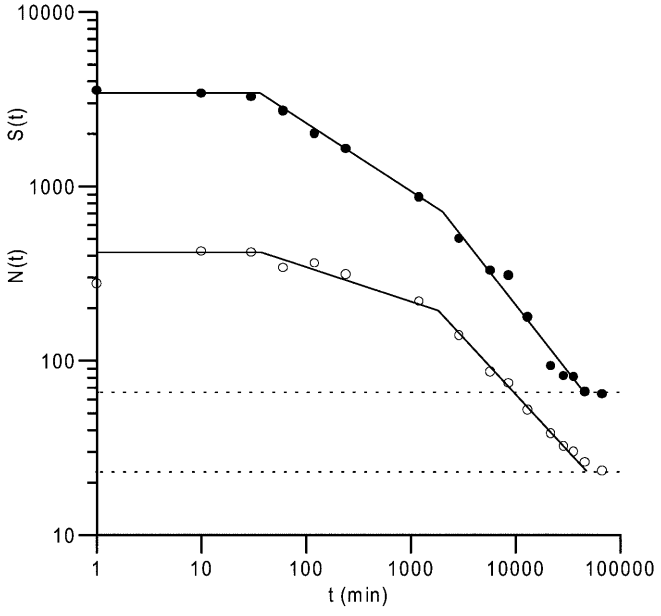

Fig. 5 Weight-average $S(t)$ (●) and number-average $N(t)$ (○) masses of the oxide grain agglomerates as a function of time for an initial PAA concentration of 3.3×10^{-4} mol/l. The *horizontal lines* show the masses $S(0)$ and $N(0)$ of the initially dispersed system

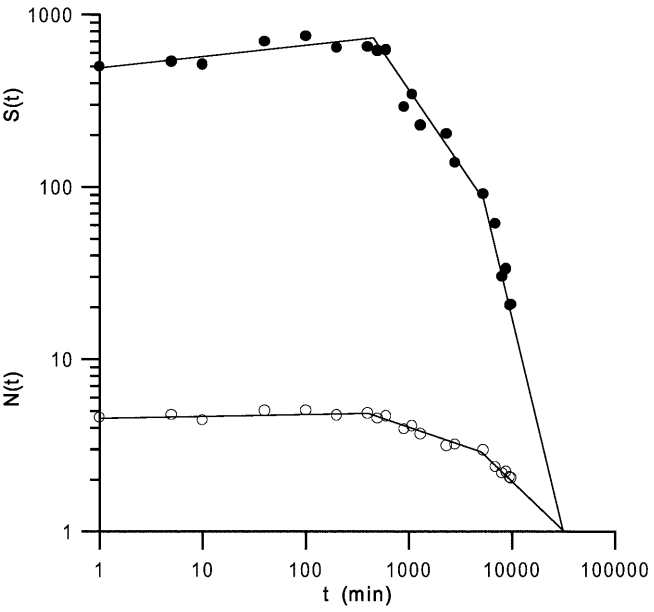

Fig. 6 $S(t)$ (●) and $N(t)$ (○) of clay fragments as a function of time. The aggregates were obtained by mixing humic acid (3×10^{-5} mol/l) and clay (0.06 g/100 g) suspended in an aqueous solution of 10^{-4} mol/l $AlCl_3$ and 10^{-3} mol/l KCl at pH 5.0

decrease. The steady state seems to result from concomitant fragmentation and aggregation processes, where fragmentation is strictly cancelled by aggregation, while the decrease in the aggregate masses indicates that the fragmentation process becomes prevailing. The theories provide rate equations of aggregate breakup, which are based on the mass distribution curves of agglomerated colloids. The rate of breakup of large aggregates, $a(n)$, is expressed by the power law (Eq. 6) and is correlated to the reduced mass frequency curve, φ, as expressed by (Eq. 10). The rate of formation of small fragments, $b(n)$, is expressed by Eq. (8) and is correlated to the mass frequency curve as expressed by Eq. (11).

The rates $a(n)$ and $b(n)$ for the synthetic and natural systems are derived from the shown in Figs. 7 and 8, respectively. The following relationships apply:

$$\text{Synthetic system} : a(\text{n}) \propto n^{0.06}, b(\text{n}) \propto n^{-1.2},$$

$$\text{Natural system} : a(n) \propto n^{0.40}, b(n) \propto n^{-2.0}.$$

There should be a major difference between the breakup modes of aggregates of the synthetic and natural systems since the rate of breakup is very slightly mass dependent in the case of the synthetic system, whereas for the natural system it strongly depends on this characteristic.

The difference in the fragmentation modes is based on the following observations:

1. For the natural system. In the domain of fast variation of $S(t)$ with time the exponent λ of the

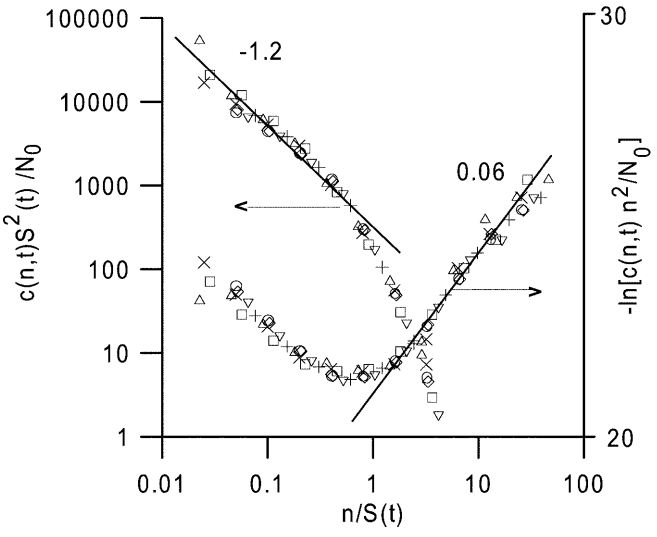

Fig. 7 Reduced mass distribution $c(n,t)S^2(t)/N_0$ (*left ordinate*) and logarithm of $c(n,t)n^2/N_0$ (*right ordinate*) of the oxide grain agglomerates as a function of the reduced mass $n/S(t)$ for an initial PAA concentration of 3.3×10^{-4} mol/l. The different *symbols* indicate data for times beyond 1000 min belonging to the fast fragmentation regime

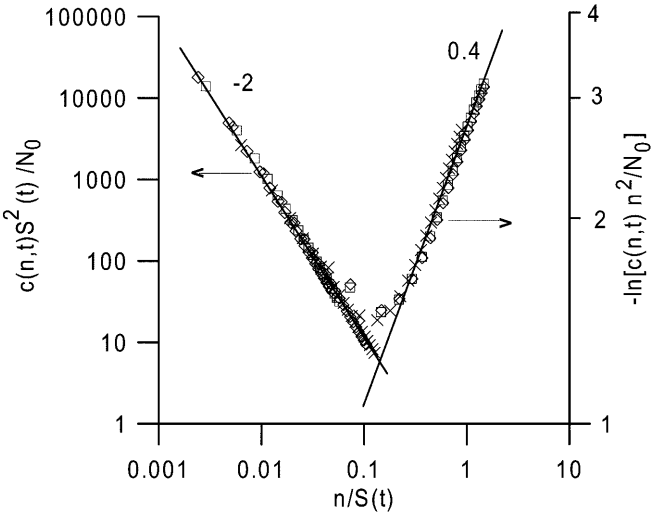

Fig. 8 $c(n,t)S^2(t)/N_0$ (*left ordinate*) and logarithm of $c(n,t)n^2/N_0$ (*right ordinate*) of the kaolinite agglomerates as a function $n/S(t)$ for an initial humic acid concentration of 3×10^{-5} mol/l and a clay dose of 0.06 g/100 g. The different *symbols* indicate data for times beyond 5000 min belonging to the fast fragmentation regime

kinetics law (Eq. 12) is equal to λ, which is derived from Eq. (10) according to the model of irreversible break up of Cheng and Redner [9, 10]. In this model, fragments issued from the breakup of larger aggregates never become engaged in succeeding aggregation processes and thus control the variation of $S(t)$. Conversely, the slower variation of $S(t)$ determined at prior times should result from concomitant aggregation and fragmentation processes.

2. For the synthetic system. In the domain of fast variation of $S(t)$ with time the slope is -0.74 and close to the value of -0.83 of $1/v$ derived from the slope of the mass frequency curve at $n/S(t) < 1$, according to Eq. (14). In the fragmentation model with the detailed balance of Ernst and van Dongen [11] aggregation prevails over fragmentation but the model may be extended to the inverse situation when the rate equations of both aggregation and fragmentation processes can be expressed using homogeneous kernels.

This difference in the fragmentation mechanism may possibly result from the chemical characteristics of the chain segments sustaining interfacial segregation. For the natural system, the reorganisation affects positively and negatively charged chain segments, both developing long-range electrical forces. It is quite possible that after dispersion induced by charge segregation the previously existing attractive interactions between stuck polymer–clay complexes cannot be established anew as far as the degree of segregation has reached a certain threshold, corresponding to the beginning of fast variation of $S(t)$. In the domain of slow variation of $S(t)$ this situation may not be established. For the synthetic system, the reorganisation affects hydrophobic–hydrophilic microdomains interacting at short distances and it is quite possible that the attractive interaction between hydrophobic microdomains belonging to different polymer–clay complexes may be renewed randomly after they have been broken, even in the domain of fast variation of $S(t)$ with time.

Conclusion

For the synthetic system, interfacial complexation of dissociated or neutral acidic groups with positively charged aluminium surface sites $-Al(OH_2^+)$ promotes the formation of neutral hydrophobic $-Al(OH_2)OOC-$ moieties. Long-range electric forces originating from surface charge are therefore precluded and the segregation affects hydrophobic and hydrophilic moieties as evidenced by changes in the electrophoretic mobility. Conversely, for the kaolinite clay basal faces which exhibit positively charged counterions, charge–charge interactions predominate and segregation affects positively and negatively charged chain segments.

Obviously, spatial segregation of amphiphilic and amphoteric sites cannot be viewed as intensive structural modifications in the chain segment distribution within the adsorbed layer. Ion-exchange reactions affecting the various Al^{n+}, K^+ or H^+ counterions of the carboxylic acid groups are able to produce similar effects.

Despite the existence of these different phenomena, fragmentation induced by adsorbed polymer develops quite similarly with the first steady-state step where aggregation and fragmentation cancel each other. The second step corresponds to a situation where fragmentation prevails, whereas the last step corresponds to irreversible fragmentation for the natural system and to coagulation/fragmentation for the synthetic system. Interpretation of these differences is based on the occurrence of the long-range effect of electrical interactions for the natural system and of the short-range effect of hydrophobic interactions for the synthetic one.

Acknowledgements The authors are grateful to G. Chauveteau (Institut Français du Pétrole) for stimulating discussions and to the Institut Français du Pétrole for partial financial support. Aluminium-Péchiney and the Laboratoire Environnement et Minéralurgie of Vandoeuvre are acknowledged for kindly providing the alumina and the kaolinite samples, respectively. E.F. would like to thank the Action Intégrée Franco-Marocaine no. 95/0873 for partially financing travel and living expenses.

References

1. Jennings JE, Knight K (1957) Proceedings of the Fourth International Conference on Soil Mechanics and Foundation Engineering. London, pp 316
2. Colom J, Wolcott AR (1967) Plant Soil 26:261
3. Dennett KE, Sturm TW, Amirtharajah A, Mahmood T (1998) Water Environ Res 70:268
4. Pierzynski GM, Sims JT, Vance GF (1994) Soils and environmental quality, Lewis, London, pp 249–261
5. Berggren D, Muller J (1995) Cosmochim Acta 20:4167
6. Chaney K, Swift RS (1984) Soil Sci 35:223
7. Chaney K, Swift RS (1986) Soil Sci 37:337
8. Ziff RM, Mc Grady ED (1985) J Phys A 18:3027
9. Cheng Z, Redner S (1988) Phys Rev Lett 60:2450
10. Cheng Z, Redner S (1990) J Phys A Math Gen 23:1233
11. Ernst MH, van Dongen PGJ (1987) Phys Rev A 36:435
12. Ringenbach E, Chauveteau G, Pefferkorn E (1993) J Colloid Interface Sci 161:223
13. Pefferkorn E, Ringenbach E, Elfarissi F (2001) Colloid Polym Sci
14. Elfarissi F, Pefferkorn E (2000) J Colloid Interface Sci 221:64
15. Theng BKG (1979) Formation and properties of clay–polymer complexes, Development in soil science series, vol 9. Elsevier, Amsterdam
16. Elfarissi F, Pefferkorn E (2000) Colloids Surf A 168:1
17. Walker PH, Hutka J (1971) Division of soils, vol 3. Technical paper no 1
18. Matthews BA, Rhodes CT (1970) J Colloid Interface Sci 32:332
19. Matthews BA, Rhodes CT (1970) J Colloid Interface Sci 32:339
20. Ives KJ (1978) The scientific basis of flocculation. Sijthoff and Noordhoff, Alphen aan den Rijn, The Netherlands, pp 165–191
21. Pefferkorn E (1995) Adv Colloid Interface Sci 56:33
22. Family F, Meakin P, Deutch JM (1986) Phys Rev Lett 57:727
23. Sorensen CM, Zhang HX, Taylor TW (1987) Phys Rev Lett 59:363
24. Meakin P (1985) J Chem Phys 83:3645
25. Botet R, Jullien R (1985) Phys Rev Lett 55:1943
26. Kolb M (1986) J Phys A Math Gen 19:L263
27. McGrady ED, Ziff RM (1987) Phys Rev Lett 58:892
28. Meakin P, Ernst MH (1988) Phys Rev Lett 60:2503
29. Elminyawi IM, Gangopadhyay S, Sorensen CM (1991) J Colloid Interface Sci 144:315
30. Pefferkorn E, Ouali L (1994) Prog Colloid Polym Sci 97:65
31. Ringenbach E, Chauveteau G, Pefferkorn E (1995) J Colloid Interface Sci 172:203
32. Joanny JF (1994) J Phys II 4:1281
33. Dobrynin AV, Rubinstein M, Joanny JF (1997) Macromolecules 30:4332
34. Ringenbach E, Chauveteau G, Pefferkorn E (1995) J Colloid Interface Sci 171:218
35. Varoqui R, Pefferkorn E (1975) J Phys Chem 79:169